

Signature of monolayer and bilayer fluctuations in the width of (Al,Ga)N/GaN quantum wells

F. Natali

RIBER S. A., 31 rue Casimir Périer, Boîte Postale 70083, 95873 Bezons Cedex, France

Y. Cordier, J. Massies, S. Veizan, B. Damilano, and M. Leroux
CRHEA-CNRS, rue B. Grégory, 06560 Valbonne, France

(Received 27 August 2008; revised manuscript received 3 November 2008; published 30 January 2009)

The photoluminescence spectra of (Al,Ga)N/GaN quantum wells grown by molecular-beam epitaxy under Ga-rich and N-rich conditions with growth interruptions at each interface exhibit several excitonic peaks, each of them corresponding to a discrete well width. This is confirmed by the excitation power dependence of the excitonic photoluminescence intensity. Well width fluctuations are then discussed in relation with atomic force microscopy and scanning tunneling microscopy images of the (Al,Ga)N surfaces. From these results, we show that the discrete well width differs by one or two molecular monolayers for growth under N-rich or Ga-rich conditions, respectively. This observation leads us to reconsider the amplitude of the built-in electric field in such structures. Contrary to what has been previously proposed in the literature, it is found identical for Ga-rich and N-rich growth conditions and equal to ~ 5 MV/cm times the AlN mole fraction.

DOI: [10.1103/PhysRevB.79.035328](https://doi.org/10.1103/PhysRevB.79.035328)

PACS number(s): 78.55.Cr, 78.66.Fd, 68.35.Ct, 78.20.Hp

I. INTRODUCTION

In the field of optoelectronic applications, the influence of the interface properties on the excitonic emission in quantum well (QW) structures has been an active topic of research during the last three decades. Since the pioneering work of Weisbuch and co-workers^{1,2} on the (Al,Ga)As/GaAs system, the role of interface roughness on the line shape of the excitonic emission has been investigated on different QW systems such as AlAs/GaAs,^{3,4} (In,Ga)As/GaAs,^{5,6} as well as (Al,Ga)Sb/GaSb.⁷ It has been shown that “molecular” monolayer (ML) fluctuations in the well thickness can be observed by low-temperature photoluminescence (PL).^{8–10} Indeed, PL shows discrete energy peaks corresponding to QW widths differing by one molecular monolayer. This molecular monolayer corresponds to half of the lattice parameter along the growth axis, i.e., one group III element atomic plane + one group V element atomic plane. One would expect to observe these fluctuations if the terrace widths are greater than the Bohr diameter of the excitons. If, on the contrary, the terrace widths are close to or smaller than the lateral extension of the exciton, the PL line shape is unique, more or less broadened depending on the details of the interfacial roughness at the exciton Bohr diameter scale.^{8–10} Contrary to the classical “square quantum well” system such as GaAs/(Al,Ga)As, the GaN/(Al,Ga)N QW system due to its growth along (0001) axis has a “triangular quantum well” scheme. This comes from the existence of huge internal electric fields, several hundreds KV/cm,^{11,12} induced by the difference in spontaneous and piezoelectric polarizations between the quantum well (GaN) and the barrier ((Al,Ga)N). Consequently, the resulting built-in electric field (F) separates both the electron and hole wave functions to each side of the QW. This means that in the GaN/(Al,Ga)N system, the electron and the hole are more sensitive to the well width fluctuation and/or alloy fluctuations than in the GaAs/(Al,Ga)As system.¹³ Furthermore, owing to the very small exciton lateral extension (in-plane Bohr diameter ~ 5 – 10 nm),^{14,15} PL should be extremely sensitive to the nanoscale interface roughness in the

(Al,Ga)N/GaN system. Although the effects of quantum confined stark effect (QSCE), QW interfaces, and alloy composition fluctuations^{11,12,14,16} have been intensively studied in this system, it is useful to note that only few reports deal with the evidence of terrace size fluctuations inferred from PL.^{17,18} This limited attention until now is quite astonishing, considering its importance from the point of view of both epitaxial growth and optoelectronic applications.

In this paper, we have revisited this phenomenon of width fluctuations via PL experiments in (Al,Ga)N/GaN QW structures grown by molecular-beam epitaxy (MBE) using either Ga-rich or N-rich growth conditions. This leads us to reconsider the amplitude of the built electric field, whose value has been the subject of controversy in the last decade. Indeed, disagreement remains about this value for (Al,Ga)N/GaN heterostructures grown under different thermodynamic conditions, i.e., either in excess of the group III metal^{16,19} or under nitrogen-rich growth conditions.^{11,12,14,20,21} We finally show that the amplitude of the electric field does not depend on the different growth conditions investigated here.

II. EXPERIMENTAL DETAILS

The QW structures were grown in a Ribier Compact 21T MBE system designed for the growth of III-nitride materials, equipped with solid effusion cells for gallium and aluminum elements, and with two nitrogen sources: an NH₃ injector (Ribier) and an N₂ radio frequency (rf) plasma source (Addon), used for N-rich growth and Ga-rich growth conditions, respectively. Indeed, using a nitrogen plasma source, it is now well established that the best (Al,Ga)N structural quality is achieved by deposition at the limit of group III metal-rich conditions (V/III flux ratio ≈ 1).^{22–24} A finite group III metal coverage (2–3 ML) is segregating at the growth front leading to a screw-type dislocation-induced spiral growth morphology consistent with a step-flow growth mode.²⁵ The presence of a high density of screw-type dislocations at the GaN (0001) surface ($> 5 \times 10^8$ cm⁻²) is inherently associated

with the growth of nitrides layers on highly lattice-mismatched substrates [here sapphire (0001)].

In the present work, the growth of (Al,Ga)N/GaN QW structures using the rf plasma cell was performed at 720 °C with a V/III ratio ≈ 1 and with growth interruptions at each interface. Indeed, without growth interruption, the excess of Al, Ga present on the surface at the beginning of QW growth favors the formation of an $\text{Al}_x\text{Ga}_{1-x}\text{N}$ alloy transient at the interface. This limits both the abruptness of the interface and the control of the well width. Thanks to the growth interruption at each interface under atomic nitrogen flux, the excess metal is consumed in part by (Al,Ga)N formation and partially by desorption, which leads to a transient of the reflection high-energy electron-diffraction (RHEED) specular spot intensity. This intensity reaches its maximum when the surface is metal free. This takes around 20 s but we have performed a longer growth interruption (~ 4 min) in order to leave the surface smoothing by atomic diffusion. On the other hand, when using NH_3 as a nitrogen source, it has been found that a V/III flux ratio > 1 and a GaN growth temperature of ~ 800 °C improve considerably the material properties both in terms of optical and structural quality.²⁶ It should be emphasized that such growth conditions are, for example, used to grow structures for high-power high-electron mobility transistor applications.^{27,28} Therefore, in the present work, the growth of (Al,Ga)N/GaN QW structures was performed at a temperature of 800 °C and under N-rich conditions (N/III flux ratio ≈ 4 , taking into account the NH_3 cracking efficiency²⁹), with growth interruptions at each interface (in order to have a comparable smoothing effect, the growth interruption time is also 4 min). Such growth conditions, close to the growth mode transition from two-dimensional (2D) island nucleation to step-flow growth mode,³⁰ lead to a surface composed of mounds in the form of truncated pyramids.³¹ The optical properties of (Al,Ga)N/GaN QWs grown in the same conditions without growth interruptions can be found elsewhere.^{14,20} It is worth noting that a GaN growth morphology identical to the one observed under Ga-rich condition using an N_2 rf plasma source can also be obtained for GaN using NH_3 . This occurs when the growth of GaN is carried out under near-stoichiometry conditions (N/III flux ratio ≈ 1), whereby the surface diffusion is enhanced compared to usual growth under excess of NH_3 .³² The different morphologies of GaN (0001) grown by MBE under Ga-rich growth and N-rich growth conditions, and their consequences on the PL properties will be discussed in detail in Sec. III of this work. PL was performed at 11 K in a closed cycle He cryostat using a frequency-doubled Ar laser for excitation ($\lambda = 244$ nm) with a spot size of 200 μm^2 , and reflectivity was recorded by shining white light from an halogen lamp onto the sample. Images of GaN (0001) surfaces were obtained both with a scanning tunneling microscope (STM) coupled under ultrahigh vacuum to a Riber nitride-dedicated molecular-beam epitaxy machine and with an *ex situ* atomic force microscope (AFM) imaging in the tapping mode.

III. RESULTS AND DISCUSSION

Figure 1 displays the PL spectra of a single 27 ML thick (1 ML = $c/2 = 2.59$ Å) GaN QW sandwiched in between

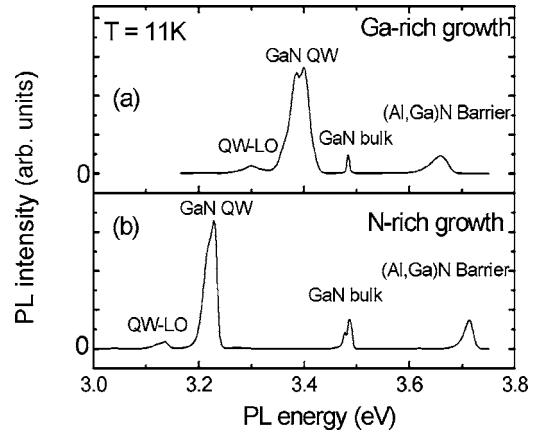


FIG. 1. Photoluminescence spectra at 11 K of $\text{Al}_x\text{Ga}_{1-x}\text{N}/\text{GaN}$ quantum well samples grown (a) under Ga-rich conditions and (b) under N-rich conditions.

$\text{Al}_{0.08}\text{Ga}_{0.92}\text{N}$ barrier layers grown under Ga-rich conditions (plasma source) and a single 25 ML thick GaN QW sandwiched in between $\text{Al}_{0.11}\text{Ga}_{0.89}\text{N}$ under N-rich conditions (NH_3 source). These thicknesses were measured using cross-section transmission electron microscopy. The QWs are encapsulated by (Al,Ga)N barriers whose thicknesses are 70 nm for the sample grown under N-rich conditions and 70 and 40 nm for the sample grown under Ga-rich conditions. Near band-edge PL from the GaN bulk and (Al,Ga)N barriers are observed together with the QW luminescence bands (lines labeled QW-LO are LO phonon replicas of the QW PL). The latter appear at a much lower energy than the band gap of GaN due to the QCSE. This effect occurs as a result of the large internal electric field present in the structure.^{11–16} It can be seen that the QW PL energy of the sample grown under N-rich condition is significantly lower than the one corresponding to the sample grown under Ga-rich condition (approximately by 165 meV). This comes from its slightly higher Al content (by 3%) and the different thicknesses of the (Al,Ga)N barriers. Taking into account both (1) the Al content difference and (2) the redistribution of the electric field between the barrier and the well in each sample (see discussion below), the well width dependence of PL energies is, for both samples, in close agreement with those determined for (Al,Ga)N/GaN quantum wells with an electric field (F) of $\sim 5.5\text{--}6.2$ MV/cm times the AlN mole fraction.^{14,20,21} For the sample grown under Ga-rich conditions [Fig. 2(a)], the PL spectrum of the QW shows the well-resolved presence of two sharp peaks, labeled $E_{\text{Ga}2}$ and $E_{\text{Ga}3}$, and two shoulders on the lower, ($E_{\text{Ga}1}$), and higher, ($E_{\text{Ga}4}$), energy side. The PL spectrum of the sample grown under N-rich condition [Fig. 2(b)] reveals both a relatively sharp emission peak ($E_{\text{N}2}$) and a shoulder on the lower energy side ($E_{\text{N}1}$). Before describing the main features of the PL spectra, let us first show that this structured QW luminescence is not due to Fabry-Pérot interferences. For that purpose, we have carried out reflectivity and PL measurements on the same wafer position (Fig. 2). It can be seen that there is no coincidence between the period of the reflectivity oscillations due to Fabry-Pérot interferences and the energy splitting between the different PL energy peaks. Actually, after Gaussian de-

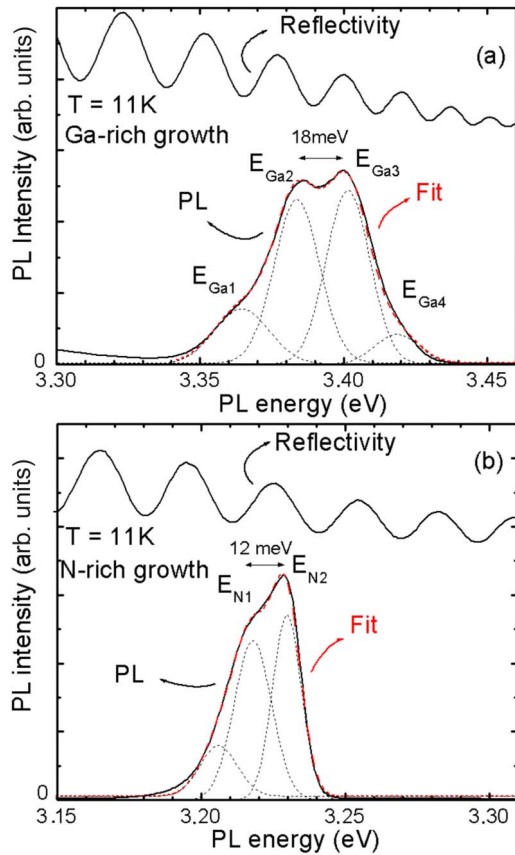


FIG. 2. (Color online) Photoluminescence and reflectivity spectra at 11 K of (Al,Ga)N/GaN quantum well samples grown (a) under Ga-rich conditions and (b) under N-rich conditions. The red lines are the fit of the PL spectra using Gaussian deconvolution (all the Gaussian components are the dotted lines).

convolution of the PL spectra (red lines in Fig. 2), the energy splitting between the different PL energy peaks remains constant (~ 18 and ~ 12 meV for the samples grown under Ga-rich and under N-rich conditions, respectively). In contrast, the energy splitting between the different reflectivity peaks decreases when approaching the GaN band edge due to the increase in the GaN refractive index. Indeed, for the sample grown under Ga-rich condition, the reflectivity energy splitting varies significantly (from 17 to 25 meV) due to the proximity of the QW emission to the GaN absorption edges. Conversely, it is almost constant (~ 30 meV) for sample grown under N-rich condition because it is relatively far from the GaN absorption edge. As a consequence of the above analysis, we can argue that the different PL peaks are not correlated with Fabry-Pérot interferences. This leads us to consider that the different PL peaks are associated to the exciton recombination lines corresponding to discrete well width fluctuations. This assignment becomes evident when looking at the dependence of the PL peak intensity as a function of the excitation power density (Fig. 3). At low excitation intensity, the main contribution to the PL comes from the wider wells (E_{Ga2}, E_{N1}). This implies that the lateral extension of the growth islands might be smaller than the diffusion length of the charge carriers (the electron and the holes). Therefore, excitons are preferably localized in the

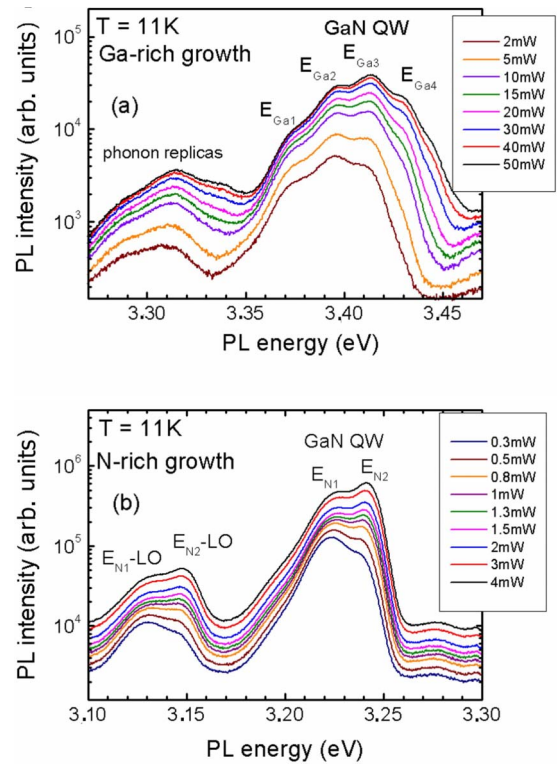


FIG. 3. (Color online) Photoluminescence spectra of (Al,Ga)N/GaN quantum well samples grown (a) under Ga-rich conditions and (b) under N-rich conditions under excitation power ranging from 2 to 50 mW and 0.3 to 4 mW, respectively.

deeper potentials corresponding to the wider well segments. It is important to note that due to the statistical distribution of well widths in the QW plane, excitonic contributions from the other wells are also distinguishable. For increasing excitation power, the number of occupied states by electrons and holes in the wider wells approaches saturation. This phenomenon occurs more easily in the wider wells because of the longer radiative lifetime of the exciton due to the larger electron-hole wave function spatial separation. As a consequence, electrons and holes start to fill the shallower potentials corresponding to thinner wells whose PL intensity significantly increases. With further increasing excitation power, this leads to an intense PL from the thinner wells due to both the increase in the carrier density and their higher oscillator strength. Each QW exhibits clearly resolved emission peaks owing to the relatively narrow PL linewidths (~ 20 meV, after Gaussian deconvolution). One can also note that the blueshift of the QW emission induced by increasing the excitation power is negligible with respect to the emission energies, which demonstrates that screening effects due to photoinduced carriers in the QWs can be excluded. It is worth noting that the phonon replica PL intensity as a function of the excitation power follows the same behavior as the one observed for the QW, as clearly seen in the case of the sample grown under N-rich condition [Fig. 3(b)]. Indeed, when the intensity of the PL peak E_{N2} increases as a function of the excitation power, its phonon replica (E_{N2-LO}), 93 meV below E_{N2} , increases as well and becomes more intense than the phonon replica of E_{N1} , E_{N1-LO} . These results well

support the hypothesis that the observed QW PL peaks correspond to thickness fluctuations in the QWs. In the case of the sample grown under Ga-rich condition, the greater number of width fluctuations (see discussion below) makes difficult a clear observation of the evolution of the phonon replica as a function of the excitation power.

The situation appears more complex when we analyze the energy splitting between the different QW related PL peaks. Let us first remind that this splitting is 18 and 12 meV for the sample grown under Ga-rich condition and the sample grown under N-rich condition, respectively. This is quite surprising because one might expect an energy splitting larger for the sample grown under N-rich condition than the one grown under Ga-rich condition. Indeed, the Al content of the sample grown under N-rich condition is higher by 3% than the QW width of the sample grown under Ga-rich condition. Then, F is larger, and the PL energy splitting should be larger.^{14,20} To understand this apparent contradiction, one should consider the surface morphology of the different samples. Generally, two distinct morphologies of GaN (0001) grown by molecular-beam epitaxy are observed, depending on the growth kinetics. When using Ga-rich growth conditions, the roughness is independent of the epitaxial layer thickness, whereas it increases with growth thickness under N-rich growth conditions.^{30,31} Furthermore, the pattern formation is different for the two regimes of growth. Under Ga-rich growth conditions, the diffusion length of adatoms is sufficiently large compared to the terrace width to allow a step-flow growth mode. In this growth regime, screw-type dislocations give rise to a spiral growth mode, which imposes both the morphological pattern and the surface roughness, as predicted by the classical model of Burton, Cabrera, and Frank.^{33,34} On the other hand, under N-rich growth conditions, the diffusion length of adatoms on the surface is reduced and becomes similar to the terrace width. This leads to a transition from step-flow dominated growth to a mixed growth mode where 2D nucleation is sufficiently active to give rise to kinetic roughening and the surface is composed of mounds in the form of a truncated pyramids.^{30,31} This is consistent with the disappearance of the RHEED oscillations during the deposition of GaN in similar conditions for growth temperature above ≈ 800 °C, meaning that a growth mode transition from 2D nucleation to step flow has been activated.³⁰ High magnification AFM scans underline the two different types of morphologies of (Al,Ga)N (0001) surfaces grown by molecular-beam epitaxy under Ga-rich [Fig. 4(a)] and under N-rich growth conditions [Fig. 4(b)]. Among the overall morphology difference, two main features can be seen on these images. First, one lattice-parameter steps corresponding to a full c vector [two molecular monolayers ($c = 5.18$ Å)] with smooth terrace edges are present under Ga-rich growth conditions, while under N-rich growth conditions one molecular monolayer steps ($c/2$) with triangular shape morphology are observed. These typical features, characteristic also of the GaN (0001) surface,³⁵ are due to the presence of two types of step edges: type A steps, normal to $\langle 1-100 \rangle$ directions, which has two dangling bonds per edge atom, and type B steps, normal to $\langle 01-10 \rangle$ directions, with only one single dangling bond per edge atom. As a consequence, the steps along the $\langle 1-100 \rangle$ directions are propagat-

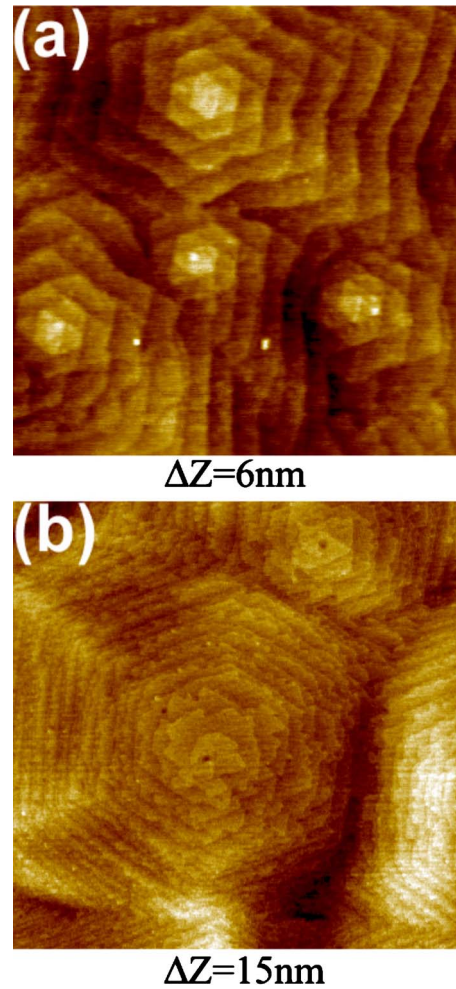


FIG. 4. (Color online) $1 \times 1 \mu\text{m}^2$ atomic force microscopy images of (Al,Ga)N/GaN quantum well samples grown (a) under Ga-rich conditions and (b) N-rich conditions.

ing faster than the steps along the $\langle 01-10 \rangle$ directions.³⁵ When the fast-growing edges reach the slow-growing edges, the terrace edges will become smooth, while the step height increases from 1 to 2 ML. Thus, if one descends the terraces along the $\langle 1-100 \rangle$ direction we will observe principally one lattice parameter (2 ML) height steps, with a constant terrace width. Such a situation occurs in the case of growth under Ga-rich conditions. From the profile of the AFM image (not shown here), the terrace width is about 30 nm and comparatively constant across the surface. In the case of the growth under N-rich conditions, the width of the terraces on the top of the mound is larger (50–60 nm) than the terraces of the sample grown under Ga-rich conditions while it decreases drastically along the mound sides [Fig. 4(b)]. It is even difficult to observe them with an AFM after descending five to six steps. To get further insights on the surface morphology at the atomic scale, STM on GaN (0001) surfaces grown on silicon substrate under N-rich conditions (V/III flux ratio of ~ 4) has been performed. We assume that the surface morphologies of GaN and $\text{Al}_{0.11}\text{Ga}_{0.89}\text{N}$ are identical due to the small Al content.³⁶ STM images of both the top of the mounds and the hillsides are shown in Figs. 5(a) and 5(b),

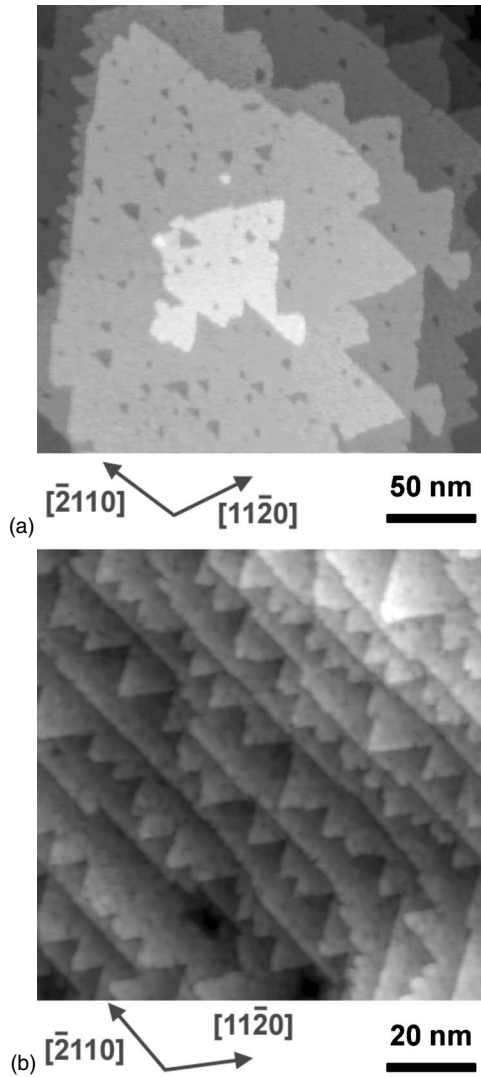


FIG. 5. (a) $300 \times 300 \text{ nm}^2$ empty states (+2 V, 0.1 nA) scanning tunneling microscopy image of the top of the mound and (b) $100 \times 100 \text{ nm}^2$ empty states (+2 V, 0.1 nA) scanning tunneling microscopy image of the hillside of GaN surface grown under N-rich regime.

respectively. As observed on the AFM image, the surface of the top of the mound is very flat with step-edge intersections forming 60° angles, giving rise to a typical triangular shape morphology. Furthermore, these terraces are much larger ($\geq 50 \text{ nm}$) than the lateral extension of the exciton. It is worth noting that only 1 ML height steps are observed on the surface, running along the $\langle 1-100 \rangle$ directions. The STM image [Fig. 5(b)] of the hillside gives details of the surface morphology, where ragged step edges alternating with right step edges are observed. The terrace width, less than 10 nm , is no longer wider than the Bohr diameter of the exciton ($\sim 10 \text{ nm}$).

The above observations lead us to consider that well width fluctuations correspond to a two molecular ML variation in the case of growth under Ga-rich conditions whereas this one is only 1 molecular height variation in the case of growth under N-rich conditions. In the latter, it is reasonable to assume that the terrace size fluctuations inferred from PL

come from the terraces on the top of the mound. Indeed, due to the scale of the roughness along the hillside, smaller in size than the exciton diameter, excitons are no longer subject to the ML size fluctuations of the QW. They are sensitive to a mean QW width. This interface is similar to the so-called pseudosmooth interface in the (Al,Ga)As/GaAs system grown on vicinal substrates.⁹ Nevertheless, a question remains: why do we observe more width fluctuations in the case of the growth under Ga-rich conditions? Let us keep in mind that the Ga-rich growth regime is associated with the presence of $\sim 2-3$ MLs of Ga atoms segregating on the surface during the growth. As a consequence, during the growth interruption under N exposure, the surface, covered with the liquid group III-metal layers, will continue to grow by consuming a part of this excess of metal. One might expect that the amount of group III-metal atoms in excess on the surface when the growth interruption starts is not homogeneously consumed. This could explain why we observe more width fluctuations in the case of the growth under Ga-rich conditions.

At this stage, it is of interest to compare the surface morphology of GaN grown by metal-organic chemical vapor deposition (MOCVD) to the one obtained by MBE. It is important to note that, as for the MBE growth of GaN, the transition from 2D island nucleation to step-flow growth mode has been observed during the growth of GaN in standard N rich conditions by MOCVD (Ref. 37) but at higher temperature ($\sim 1000^\circ \text{C}$ instead of 800°C). It is frequently reported that the surface of GaN grown by MOCVD exhibits single molecular high steps for the step-flow growth mode.³⁴ But, in contrast, for a dominant step-flow growth mode too, it has also been reported that steps of 2 ML in height are observed while under growth conditions where 2D nucleation is active, steps of single ML in height are present.³⁸ The latter observation agrees with the present results obtained for MBE growth of GaN under N-rich conditions. It is worth noting that the well width fluctuations inferred by PL in GaN/(AlGa)N QW grown by MOCVD reported by Haratizadeh and co-workers^{17,18} correspond to 2 ML in height.

Let us now examine the QW energy transitions of the samples grown under Ga-rich and N-rich conditions as a function of the well thickness. We have considered that the nominal thicknesses of 27 and 25 ML correspond to the more intense PL peaks, $E_{\text{Ga}2}$ and $E_{\text{N}1}$, at low excitation power for the GaN/ $\text{Al}_{0.08}\text{Ga}_{0.92}\text{N}$ QW and GaN/ $\text{Al}_{0.11}\text{Ga}_{0.89}\text{N}$ QW, respectively. Figure 6 displays the experimental and calculated well width dependence of the PL energies. The QW transition energies were modeled using the envelope-function formalism, including the electric field as a fitting parameter. The material parameters used in the calculation are given in Ref. 20. The results are displayed as solid lines in Fig. 6, showing that a good agreement with the experiment is obtained for the range of well widths investigated. It is worth noting that the calculations are corrected for the localization energies, which we determine experimentally from the S-shape dependence of the QW energies as a function of the temperature.¹² Furthermore, as the electric field induced by the polarization discontinuities at interfaces redistributes between wells and barriers, the field in the wells is reduced from its value expected for infinite barriers by a geometrical factor. We re-

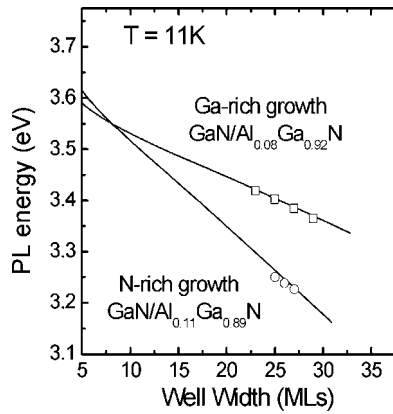


FIG. 6. Quantum well luminescence energies of the (Al,Ga)N/GaN quantum well samples grown under Ga-rich conditions (open squares) and N-rich conditions (open circles) as a function of well thickness. The solid lines are the calculated energies.

member that the QWs are encapsulated by (Al,Ga)N barriers whose thicknesses are 70 nm for the sample grown under N-rich condition and 70 and 40 nm for the sample grown under Ga-rich condition. The internal field, approximated by a constant effective field inside the well, is modified by a ratio $L_b/(L_b+w)$, where L_b is the thickness of the barrier layer and w is the QW width.^{20,39} Taking into account this geometrical factor, we determine an electric field of $\sim 400 \pm 30$ and 740 ± 40 KV/cm for the sample grown under Ga-rich conditions and under N-rich conditions, respectively. This corresponds to an electric field of 5 MV/cm times the AlN mole fraction and 6.7 MV/cm times the AlN mole fraction for the sample grown under Ga-rich conditions and under N-rich conditions, respectively. Such values are in good agreement with the previous values reported in the literature in the case of samples grown under N-rich conditions (~ 5.5 – 6.2 MV/cm times the AlN mole fraction).^{11,14,20,21,40} Therefore, the magnitude of the electric field of the sample grown under Ga-rich conditions is significantly smaller, by approximately a factor of ~ 1.6 , than the value reported previously for comparable structures grown under Ga-rich conditions (for an AlN mole fraction ranging from 0.072 to 0.172).¹⁶ Value of built-in electric field as large as ~ 9.2 MV/cm times the AlN mole fraction in structures grown under Ga-rich conditions has also been reported for AlN/GaN quantum wells.¹⁹ As a consequence, the present set of results, even if far from exhaustive, clearly shows that we must question the determination of the built-in electric field from the PL energy peaks as a function of the well widths. One of the reasons put forward in the literature to explain the difference in the reported electric field magnitude has been the large variation in the growth temperature used by the various groups. The present study shows that the amplitude of the built-in electric field does not appear very sensitive to the growth temperature (about 100 °C of difference between the growths under N-rich and Ga-rich conditions).

Another point should be discussed now. The present study shows that (Al,Ga)N/GaN QWs grown under N-rich condition and with interruptions at each interface exhibit well width fluctuations in the PL spectrum. Such a situation is

very similar to what occurs in the (Al,Ga)As/GaAs system, where growth interruptions involve the surface migration of the Ga and/or Al adatoms leading to the formation of large molecular monolayer height islands giving rise to discrete PL peaks.^{41,42} It is important to mention that we have already reported extensively on (Al,Ga)N/GaN QWs grown under N-rich conditions but without growth interruptions at each interface and we did not observe any resolved well width fluctuations in the PL spectra for QW widths ranging from 4 to 30 molecular ML and Al content lower than <0.16 .^{12,14,20,39} On the other hand, well width fluctuations have been observed for high Al contents (>0.25) and thick QWs (30 ML) grown under N-rich conditions.^{14,20,39} In this particular case, the morphology pattern of the (Al,Ga)N surface has a propensity to give rise to a spiral growth mode similar to the one resulting from the Ga-rich growth conditions of GaN.³⁶ It is further worth noting also that, for a given QW width and Al content, we observe that the QW luminescence energy of a sample grown under N-rich conditions with interruption at each interface is the same as the sample grown under N-rich conditions without growth interruptions.²⁰ The magnitude of the electric field of the (Al,Ga)N/GaN QW sample grown under N-rich conditions with interruption at each interface is 6.7 MV/cm times the AlN mole fraction. This is almost identical with the electric field presents in similar (Al,Ga)N/GaN QW structures grown without growth interruption.

IV. CONCLUSION

The optical properties of (Al,Ga)N/GaN quantum wells grown by molecular-beam epitaxy under Ga-rich and N-rich conditions with growth interruptions at each interface have been studied. PL spectra exhibit several exciton peaks that we attribute to the well width fluctuations. It is suggested that the different surface morphologies, imposed by the different thermodynamic growth conditions, lead to well width fluctuations corresponding to two molecular monolayer height fluctuations in the case of growth under Ga-rich conditions and one molecular monolayer height fluctuation in the case of growth under N-rich conditions. Thanks to the PL spectrum which shows well-resolved QW luminescence peaks, a built-in electric field of ~ 5 MV/cm times the AlN mole fraction is determined for the sample grown under Ga-rich conditions. This magnitude of the electric field is in good agreement with the previous value reported in the literature in the case of similar samples grown under N-rich conditions (~ 5.5 – 6.2 MV/cm times the AlN mole fraction).^{11,14,20,21,40} This result allows us to conclude that the growth conditions do not seem to play a major role in the magnitude of the polarization field in wurtzite (Al,Ga)N/GaN heterostructures.

ACKNOWLEDGMENTS

F.N. would like to thank O. Tottreau for many helpful and valuable discussions about AFM and TEM and P. Venegues for TEM measurements. This work was carried out at RIBER GaN Process Technology Center (PTC) in Valbonne, France, in collaboration with the CRHEA-CNRS laboratory.

- ¹C. Weisbuch, R. C. Miller, R. Dingle, A. C. Gossard, and W. Wiegmann, *Solid State Commun.* **38**, 709 (1981).
- ²C. Weisbuch, R. Dingle, P. M. Petroff, A. C. Gossard, and W. Wiegmann, *Appl. Phys. Lett.* **38**, 840 (1981).
- ³D. Gammon, B. V. Shanabrook, and D. S. Katzer, *Phys. Rev. Lett.* **67**, 1547 (1991).
- ⁴J. Zhang, P. Dawson, J. H. Neave, K. J. Hugill, I. Galbraith, P. N. Fawcett, and B. A. Joyce, *J. Appl. Phys.* **68**, 5595 (1990).
- ⁵J. Leymarie, C. Monier, A. Vasson, A.-M. Vasson, M. Leroux, B. Courboulès, N. Grandjean, C. Deparis, and J. Massies, *Phys. Rev. B* **51**, 13274 (1995).
- ⁶J. R. Botha and A. W. R. Leitch, *J. Cryst. Growth* **169**, 629 (1996).
- ⁷C. Bocchi, L. Lazzarini, M. Minelli, L. Nasi, and E. Kh. Mukhamedzhanov, *J. Appl. Phys.* **96**, 3110 (2004).
- ⁸B. Deveaud, J. Y. Emery, A. Chomette, B. Lambert, and M. Baudet, *Appl. Phys. Lett.* **45**, 1078 (1984).
- ⁹J. Massies, C. Deparis, C. Neri, G. Neu, Y. Chen, B. Gil, P. Auvray, and A. Regreny, *Appl. Phys. Lett.* **55**, 2605 (1989).
- ¹⁰M. Tanaka and H. Sakaki, *J. Cryst. Growth* **81**, 153 (1987).
- ¹¹Jin Seo Im, H. Kollmer, J. Off, A. Sohmer, F. Scholz, and A. Hangleiter, *Phys. Rev. B* **57**, R9435 (1998).
- ¹²M. Leroux, N. Grandjean, M. Laügt, J. Massies, B. Gil, and P. Lefebvre, *Phys. Rev. B* **58**, R13371 (1998).
- ¹³M. Gallart, P. Lefebvre, A. Morel, T. Taliércio, B. Gil, J. Allegre, H. Mathieu, B. Damilano, N. Grandjean, and J. Massies, *Phys. Status Solidi A* **183**, 61 (2001).
- ¹⁴F. Natali, D. Byrne, M. Leroux, D. Damilano, F. Semond, A. Le Louarn, S. Veizian, N. Grandjean, and J. Massies, *Phys. Rev. B* **71**, 075311 (2005).
- ¹⁵P. Bigenwald, P. Lefebvre, T. Bretagnon, and B. Gil, *Phys. Status Solidi B* **216**, 371 (1999).
- ¹⁶J. Simon, R. Langer, A. Barski, and N. T. Pelekanos, *Phys. Rev. B* **61**, 7211 (2000).
- ¹⁷H. Haratizadeh, B. Monemar, Plamen P. Paskov, Per Olof Holtz, E. Valcheva, P. Persson, M. Iwaya, S. Kamiyama, H. Amano, and I. Akasaki, *Phys. Status Solidi B* **244**, 1727 (2007).
- ¹⁸E. Valcheva, S. Dimitrov, B. Monemar, H. Haratizadeh, P. Persson, H. Amano, and I. Akasaki, *Acta Phys. Pol. A* **112**, 395 (2007).
- ¹⁹C. Adelman, E. Sargiannidou, D. Jalabert, Y. Hori, J. L. Rouvière, B. Daudin, S. Fanget, C. Bru-Chevalier, T. Shibata, and M. Tanaka, *Appl. Phys. Lett.* **82**, 4154 (2003).
- ²⁰N. Grandjean, D. Damilano, S. Dalmaso, M. Leroux, S. Laugt, and J. Massies, *J. Appl. Phys.* **86**, 3714 (1999).
- ²¹N. Grandjean, D. Damilano, J. Massies, G. Neu, M. Teisseire, I. Grzegory, S. Porowski, M. Gallart, P. Lefebvre, B. Gil, and M. Albrecht, *J. Appl. Phys.* **88**, 183 (2000).
- ²²C. Adelman, J. Brault, D. Jalabert, P. Gentile, H. Mariette, G. Mula, and B. Daudin, *J. Appl. Phys.* **91**, 9638 (2002).
- ²³B. Heying, I. Smorchkova, C. Poblentz, C. Elsass, P. Fini, S. P. DenBaars, U. K. Mishra, and J. S. Speck, *Appl. Phys. Lett.* **77**, 2885 (2000).
- ²⁴G. Koblmüller, J. Brown, R. Averbek, H. Riechert, P. Pongratz, and J. S. Speck, *Jpn. J. Appl. Phys., Part 2* **44**, L906 (2005).
- ²⁵G. Koblmüller, S. Fernández-Garrido, E. Calleja, and J. S. Speck, *Appl. Phys. Lett.* **91**, 161904 (2007).
- ²⁶N. Grandjean, M. Leroux, J. Massies, M. Mesrine, and M. Laugt, *Jpn. J. Appl. Phys., Part 1* **38**, 618 (1999).
- ²⁷R. Behtash, H. Tobler, M. Neuburger, A. Schurr, H. Leier, Y. Cordier, F. Semond, F. Natali, and J. Massies, *Electron. Lett.* **39**, 626 (2003).
- ²⁸Y. Cordier, F. Semond, P. Lorenzini, N. Grandjean, B. Damilano, J. Massies, V. Hoel, A. Minko, N. Vellas, C. Gaquiere, J. C. DeJaeger, B. Dessertene, S. Cassette, M. Surrugue, D. Adam, J. C. Grattapain, R. Aubry, and S. Delage, *J. Cryst. Growth* **251**, 811 (2003).
- ²⁹M. Mesrine, N. Grandjean, and J. Massies, *Appl. Phys. Lett.* **72**, 350 (1998).
- ³⁰N. Grandjean and J. Massies, *Appl. Phys. Lett.* **71**, 1816 (1997).
- ³¹S. Veizian, F. Natali, F. Semond, and J. Massies, *Phys. Rev. B* **69**, 125329 (2004).
- ³²S. Veizian, J. Massies, F. Semond, and N. Grandjean, *Mater. Sci. Eng., B* **82**, 56 (2001).
- ³³W. K. Burton, N. Cabrera, and F. C. Frank, *Philos. Trans. R. Soc. London, Ser. A* **243**, 299 (1951).
- ³⁴B. Heying, E. J. Tarsa, C. R. Elsass, P. Fini, S. P. DenBaars, and J. S. Speck, *J. Appl. Phys.* **85**, 6470 (1999).
- ³⁵M. H. Xie, S. M. Seutter, W. K. Zhu, and L. X. Zheng, Huasheng Wu, and S. Y. Tong, *Phys. Rev. Lett.* **82**, 2749 (1999).
- ³⁶F. Natali, Ph.D. thesis, Université de Nice Sophia Antipolis, 2003.
- ³⁷G. B. Stephenson, J. A. Eastman, C. Thompson, O. Auciello, L. J. Thompson, A. Munkholm, P. Fini, S. P. DenBaars, and J. Speck, *Appl. Phys. Lett.* **74**, 3326 (1999).
- ³⁸T. Nishida, N. Maeda, T. Akasaka, and N. Kobayashi, *J. Cryst. Growth* **195**, 41 (1998).
- ³⁹M. Leroux, N. Grandjean, J. Massies, B. Gil, P. Lefebvre, and P. Bigenwald, *Phys. Rev. B* **60**, 1496 (1999).
- ⁴⁰N. Grandjean, J. Massies, and M. Leroux, *Appl. Phys. Lett.* **74**, 2361 (1999).
- ⁴¹M. A. Herman, D. Bimberg, and J. Christen, *J. Appl. Phys.* **70**, R1 (1991).
- ⁴²T. R. Block, D. P. Neikirk, and B. G. Streetman, *J. Vac. Sci. Technol. B* **10**, 832 (1992).